Journal of Materials Chemistry C

Accepted Manuscript

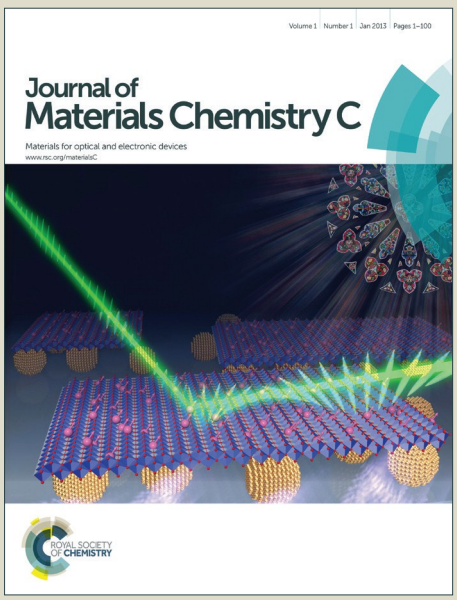

ROYAL SOCIETY OF CHEMISTRY

www.rsc.org/materialsC

Journal Name

ARTICLE

Study on $K_2SbF_2Cl_3$ as a New mid-IR Nonlinear Optical Material: New Synthesis and Excellent Properties†

Received 00th January 20xx,
Accepted 00th January 20xx

DOI: 10.1039/x0xx00000x

www.rsc.org/

Yin Huang,[a, b] Xianggao Meng,[c] Pifu Gong,[d] Zheshuai Lin,[*d] Xingguo Chen[a] and Jingui Qin[*a]

To search for new nonlinear optical (NLO) material to be used in the mid-IR region with excellent comprehensive performance including high laser damage threshold (LDT), $K_2SbF_2Cl_3$ has been synthesized by the hydrothermal method, and its potential as such new material isevaluated for the first time. Its powders show phase-matchable second harmonic generation (SHG) response of approximately 4 times as strong as that of KH_2PO_4 (KDP). Its optical band gap is 4.01eV which is much wider than the band gaps of the currently commercialised IR NLO crystals. This means that $K_2SbF_2Cl_3$ will exhibit much higher LDT. Its powders also exhibit excellent transparency in the range of 0.31-14 μm and a good thermal stability. The relationship between the composition, crystal structure and properties is discussed. These results indicate that $K_2SbF_2Cl_3$ is a promising candidate for IR NLO materials.

Introduction

Second-order nonlinear optical (NLO) crystal materials have played a very important role in the laser technology, such as laser frequency conversion, optical parameter oscillators, and signal communication.[1]In the past decades, many important NLO crystals have been found in the UV and visible regions, such as β-BaB_2O_4 (BBO), LiB_3O_5 (LBO), KH_2PO_4 (KDP), $KTiOPO_4$ (KTP) and $LiNbO_3$ (LN) etc.[2] But, in the IR region, some currently commercialised NLO crystals such as $AgGaS_2$, $AgGaSe_2$ and $ZnGeP_2$[3] have suffered from low LDT, and their applications for laser communication and high power confront are heavily hindered. It has been believed that small band gaps of these semiconductive chalcogenides are intrinsic reason for their low LDT. Therefore, searching for new IR NLO crystals with wideband gaps and the excellent comprehensive performances has become one of the great challenges in this field.

In the last decade or so, our group have investigated the suitability of halides as such new materials because they usually possess the relatively large band gaps which are beneficial to improve the laser damage threshold in crystal. Some new potential IR NLO materials such as $CsGeCl_3$, $CsCdBr_3$, SbF_3, $NaSb_3F_{10}$, $Cs_2Hg_3I_8$, $HgBr_2$, Hg_2BrI_3, $Cs_2HgI_2Cl_2$, HgBrI, Hg_2Br_3I, $Rb_2CdBr_2I_2$, β-HgBrCl, $Hg_6P_3In_2Cl_9$ and $Hg_8As_4Bi_3Cl_{13}$ have been developed in this regard.[4]

In this work, we pay our special attention to antimony halides, since antimony is a relatively strong metal and its compounds with F and Cl must exhibit wide band gaps so as to show high LDT. Meanwhile the Sb^{3+}cationwith a lone pair of electrons is beneficial for NLO performance due to easy electron polarisation. It was found in the literature that $K_2SbF_2Cl_3$ and Na_2SbF_5 have the same space group ($P2_12_12_1$).[5] We are interested in these two halides containing fluoride and chloride anions because not only their crystals belong to noncentrosymmetric (NCS) crystal system but also they both should possess very wide band gaps so as to show high LDT values. Na_2SbF_5has been reported to show very weak second order NLO property, and its powder SHG effect was only 0.4 times that of KDP. The single crystal structure of $K_2SbF_2Cl_3$ was firstly reported by Zemnukhova et al. in 1998. But to the best of our knowledge, there has been no report about its nonlinear optical property. We have a strong feeling that $K_2SbF_2Cl_3$ should exhibit stronger SHG effect than Na_2SbF_5while keep relatively wide band gap, since within our experience, partially replacing fluoride anions in halides by chloride anions will enhance the electron polarization and SHG effect will be stronger. So we decide to make our effort to investigate $K_2SbF_2Cl_3$for its potential as new mid-IR NLO material. First we synthesized it by hydrothermal reaction which is different from the literature where it was synthesised by conventional reaction in normal solution. Then we measured the single crystal structure of $K_2SbF_2Cl_3$again and investigated its NLO property and some other important properties. All the results indicate that, as we expected, $K_2SbF_2Cl_3$ showed much stronger SHG effect and is a new promising candidate for mid-IR NLO materials. In this paper, we report its new synthesis, crystal structure, and various properties as well as the

[a]Department of Chemistry, Wuhan University, Wuhan 430072, China, E-mail: jgqin@whu.edu.cn
[b]Hubei Institute of Aerospace Chemotechnology, Xiangyang 441003, China
[c]College of Chemistry, Central China Normal University, Wuhan 430079, China
[d]Beijing Center for Crystal R&D, Technical Institute of Physics and Chemistry, Chinese Academy of Sciences, Beijing 100190, China, E-mail: zslin@mail.ipc.ac.cn
† Footnotes relating to the title and/or authors should appear here.
Electronic Supplementary Information (ESI) available: [XRD, the structure of K2SbF2Cl3, and the coordination structure of K]. See DOI: 10.1039/x0xx00000x

relationship between the composition, crystal structure and properties through theoretical calculations.

Experimental

Materials and Instruments

All the chemicals were analytically pure from commercial sources and used without further purification.

Powder X-ray diffraction (XRD) patterns of polycrystalline material were collected on a Bruker D8 Advanced diffractometer with Cu-K_α radiation (λ = 1.5418 Å) in the range of 10°-70° (2θ) at a scanning rate of 6°/min.

The optical transmission spectra in the mid-IR region were recorded on a NICOLET 5700 Fourier-transformed infrared (FT-IR) spectrophotometer in the 4000-700 cm^{-1} region (2.5-14 μm) using the attenuated total reflection (ATR) technique with a germanium crystal.

The UV-vis diffuse reflectance spectra were measured on a Varian Cary 5000 UV-vis-NIR spectrophotometer in the region of 200-1000 nm. A $BaSO_4$ plate was used as the standard (100% reflectance), on which the finely ground samples from the crystals were coated. The absorption spectrum was calculated from the reflectance spectra using the Kubelka-Munk function: $\alpha/S = (1-R)^2/2R$,[6] where α is the absorption coefficient, S is the scattering coefficient, and R is the reflectance.

The measurements of second harmonic generation (SHG) were carried out on the sieved powder samples by using the Kurtz and Perry method with a 1064 nm Q-switched Nd: YAG laser.[7] Microcrystalline KDP served as the standard.

The thermogravimetric analysis (TGA) was carried out with a Netzsch STA 449c analyzer. The crystal sample was added into an Al_2O_3 crucible and heated from 30 °C to 800 °C at a heating rate of 10 K/min under flowing N_2.

Synthesis

The compound $K_2SbF_2Cl_3$ can be synthesized by hydrothermal method. Stoichiometric amounts of KF (20mmol, 1.1620 g) and $SbCl_3$ (10mmol, 2.2812 g) and 2 mL aqueous hydrochloric acid (HCl: H_2O=1: 1) were sealed in a 23 mL Teflon-lined autoclave. The autoclave was gradually heated to 180°C, held for one day, and cooled naturally to room temperature. The product was washed with ethanol and then dried in air (2.9959 g, 87 %). The phase purity was checked by powder XRD (Fig. S1, ESI†). The measured powder X-ray diffraction patterns are in good agreement with the calculated patterns based on the single crystal structures of thetitle compounds, showing that no impurities were observed.

Single-Crystal Structure Determination

Single crystal of $K_2SbF_2Cl_3$ with dimensions of 0.10×0.10×0.10 mm^3 was selected and used for single-crystal diffraction experiment. Data sets were collected using a Bruker APEX-II CCD diffractometer equipped with a CCD detector (graphite-monochromated Mo-K_α radiation λ = 0.71073 Å) at 296(2) K. Data sets reduction and integration were performed using the software package *SAINT PLUS*.[8] The crystal structure is solved by direct methods and refined using the *SHELXTL 97* software package.[9] The crystal data and structure refinement for $K_2SbF_2Cl_3$ are listed in Table 1 and the selected bond distances are summarized in Table 2. The collected crystal data (with CCDC numbers 997373) are consistent with the data reported in the literature.[5]

Table. 1 Crystal data and structure refinement for $K_2SbF_2Cl_3$.

Formula	$K_2SbF_2Cl_3$
Formula weight	344.30
Temperature (K)	296(2) K
Crystal system	Orthorhombic
Space group	$P2_12_12_1$
a (Å)	7.6320(11)
b (Å)	8.1788(11)
c (Å)	12.7931(17)
V ($Å^3$)	798.55(19)
Z	4
Density (calculated) ($g \cdot m^{-3}$)	2.864
Absorption coefficient (mm^{-1})	5.438
F(000)	632
Crystal size (mm^3)	0.10 x 0.10 x 0.10
Reflections collected	6059
Independent reflections	1997 [R(int) = 0.0347]
Data / restraints / parameters	1997 / 0 / 73
Goodness-of-fit on F^2	1.013
Final R indices [I>2sigma(I)][a]	R_1 = 0.0241, wR_2 = 0.0381
R indices (all data)	R_1 = 0.0282, wR_2 = 0.0398

[a] $R_1 = \sum||F_o| - |F_c|| / \sum|F_o|$, $wR_2 = \{\sum[w(F_o^2 - F_c^2)^2]/\sum w[(F_o)^2]^2\}^{1/2}$.

Table. 2 Selected bond distances (Å) of $K_2SbF_2Cl_3$.

Bond Distances	Bond Distances
Sb(1)-F(1) 1.983(2)	Sb(1)-Cl(1)2.6490(11)
Sb(1)-F(2) 1.958(2)	Sb(1)-Cl(2) 2.5613(11)
	Sb(1)-Cl(3)2.8893(11)

Computational Method

To investigate the origin of the difference in NLO effects, the first-principles electronic structure calculations for $K_2SbF_2Cl_3$ and Na_2SbF_5 crystals were performed by the plane-wave pseudopotential method[10] implemented in the CASTEP package[11] based on the density functional theory (DFT).[12] The optimized normal-conserving pseudopotentials[13] allow us to usea small plane-wave basis set without compromising the accuracy required by our study, and the local density approximation (LDA)[14] with CA-PZ functionals are chosen to describe the exchange and correlation (XC) potentials. The cutoff energy for the plane wave basis was set to be 900eV. The K-points sampling in the Brilliouin zone were set to be 3×2×2 and 4×2×2, according to the Monkhorst-Pack scheme.[15]

Our tests revealed that the above computational parameters are sufficiently accurate for the present purpose.

It is well acknowledged that the DFT calculations with the XC functional always underestimate the energy band gap of crystals. For calculating the optical coefficients, thus a scissors operator[16]was introduced to shift up all the conduction bands to agree with the measured band gap. Based on the electronic structures, the refractive indices and birefringence can be predicted by considering the electronic transition between valance band (VB) and conduction band (CB)[17]and the second-order susceptibility $\chi^{(2)}$, i.e., the SHG coefficient d_{ij}, can be calculated by the formula developed by Lin et al.[18]

In order to analyze the contribution of an ion (or ionic group) to the *n*-th order susceptibility $\chi^{(n)}$, a real-space atom-cutting technique[18] is adopted. Within this method the contribution of ion *A* to the *n*-th order susceptibility (denoted as $\chi^{(n)}(A)$) is obtained by cutting all ion except *A* from the original wave functions, i.e., $\chi^{(n)}$(A)= $\chi^{(n)}$(all ions except *A* are cut).

Results and Discussions

Crystal Structural Descriptions

Single crystal structural analysis indicates that $K_2SbF_2Cl_3$ crystallizes in orthorhombic space group $P2_12_12_1$. The asymmetric unit contains two crystallographically independent K atoms, one independent Sb atom, two independent F atoms, and three independent Cl atoms. Each Sb atom is five-coordinated by two F atoms and three Cl atoms to form the $[SbF_2Cl_3]^{2-}$ square pyramid (Fig. 1). The two Sb-F distances are 1.983(2) and 1.958(2) Å, respectively. The Sb-Cl distances are ranging from 2.5613(11) to 2.8893(11) Å. The arrangement of $[SbF_2Cl_3]^{2-}$ groups is shown in Fig. 2. Although $K_2SbF_2Cl_3$ is not crystallized in one of ten polar point groups (1, 2, 3, 4, 6, m, mm2, 4mm, 3m, 6mm), its crystal obtained in the chiral space group $P2_12_12_1$ demonstrates the NCS spatial packing. First, from the coordination environment around metal centre Sb (Fig.1), it can be easily seen that $[SbF_2Cl_3]^{2-}$ group is a NCS group. Secondly, the arrangement of $[SbF_2Cl_3]^{2-}$ groups in three dimensional space is not cetrosymmetric (Fig. 2), and it is this arrangement that makes the crystal possess the NCS structure. As a result, $K_2SbF_2Cl_3$ should be able to exhibit a relatively strong SHG response.

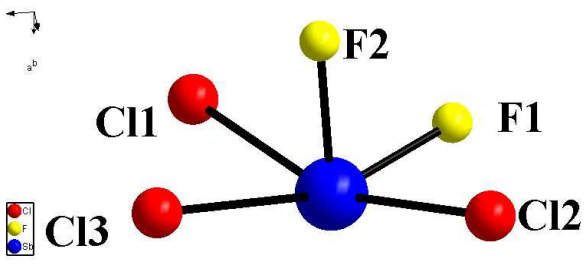

Fig.1 The structure of $[SbF_2Cl_3]^{2-}$ group.

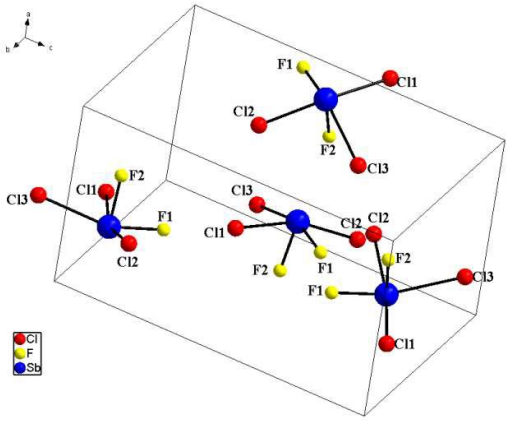

Fig. 2 The arrangement of $[SbF_2Cl_3]^{2-}$ groups.

ATR-FTIR and UV-vis Spectra

The ATR-FTIR spectrum of $K_2SbF_2Cl_3$ indicates that the transparent region of its powders is in the range of 4000-700 m^{-1} (2.5-14μm) (Fig.3). The UV-vis absorption spectrum and optical diffuse reflectance spectrum of $K_2SbF_2Cl_3$ show that its absorption edge is at 309 nm. This indicates that the optical band gap of $K_2SbF_2Cl_3$ is 4.01 eV (Fig.4) which is much higher than that of commercially available IR NLO crystal $AgGaS_2$ (2.75 eV). As it is well known that the size of the band gap is an intrinsic factor to determine the value of the LDT, it is believed that $K_2SbF_2Cl_3$ should exhibit a much higher LDT than $AgGaS_2$.

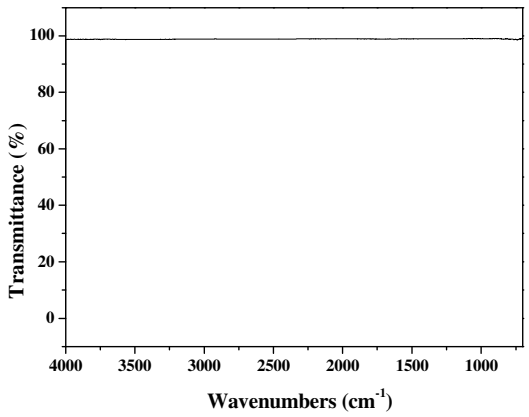

Fig.3 ATR-FTIR spectrum of $K_2SbF_2Cl_3$.

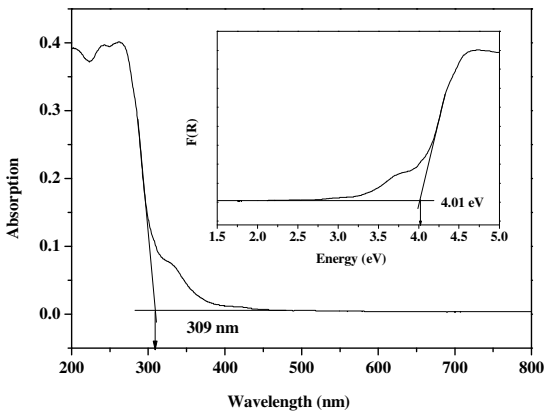

Fig.4 UV-visabsorption spectrum; and the inset is optical diffuse reflectance spectrum of $K_2SbF_2Cl_3$.

NLO Property

Powder SHG measurements using 1064 nm radiation revealed that $K_2SbF_2Cl_3$showed SHG efficiencies approximately of about 4 times as strong as that of KDP. The tendency of the curve indicates that $K_2SbF_2Cl_3$ belongs to the phase-matchable class, which is a very important character of NLO material for the laser harmonic generation (Fig.5).

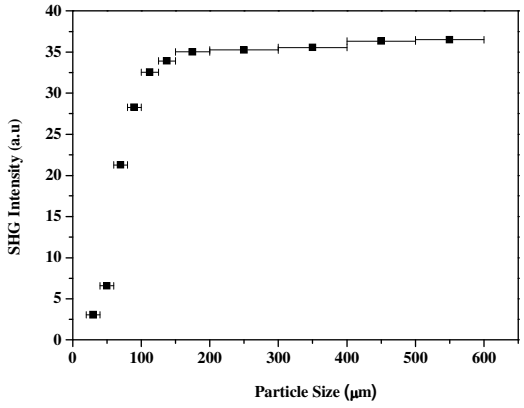

Fig. 5 The phase-matching curve of $K_2SbF_2Cl_3$.

Theoretical Calculations

Electronic structures

Fig. 6(a) and (b) show the first-principles electronic band structures of $K_2SbF_2Cl_3$ and Na_2SbF_5 along the lines of high symmetry points in the Brillouin zone, respectively. Clearly, $K_2SbF_2Cl_3$ is a direct gap crystal, while Na_2SbF_5 is an indirect gap crystal with the energy band gap at G point 0.6 eV larger than the indirect gap. Meanwhile, Fig. 7 display the partial density of states (PDOS) projected on the constitutional atoms in both crystals, from which the following electronic characteristics can be deduced: (i) The region lower than -7 eV are composed of the localized inner-shell state with K 3s3p (Na 2s2p), Sb 5s, Cl 3s and F 2s orbitals, which have little interaction with the neighbor atoms. (ii) The upper part of VB and the bottom of the CB are mainly composed of the orbitals of Sb 5s5p, F 2p and Cl 3p orbitals in $K_2SbF_2Cl_3$ and Sb 5s5p, F 2p orbitals in Na_2SbF_5, indicating that the states on the both side of the band gap are mainly contributed from the $(SbF_2Cl_3)^{2-}$ and $(SbF_5)^{2-}$ group.Since the optical response of a crystal mainly originates from the electronic transitions between the VB and CB states close to the band gap,[19] the two groups determine the optical properties in both crystals, in accordance with the anionic group theory proposed by Chen[20] for the ultraviolet NLO crystals.

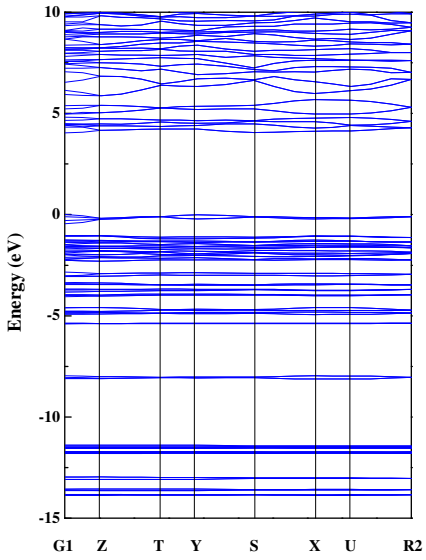

(a)

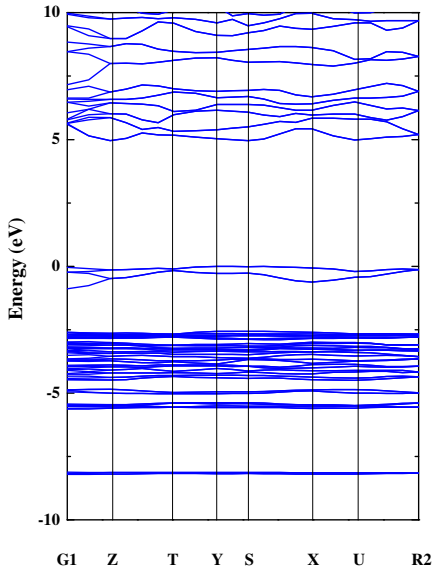

(b)

Fig. 6 The electronic band structure of (a) $K_2SbF_2Cl_3$ and (b)Na_2SbF_5along the lines of high symmetry points in the Brillouin zone.

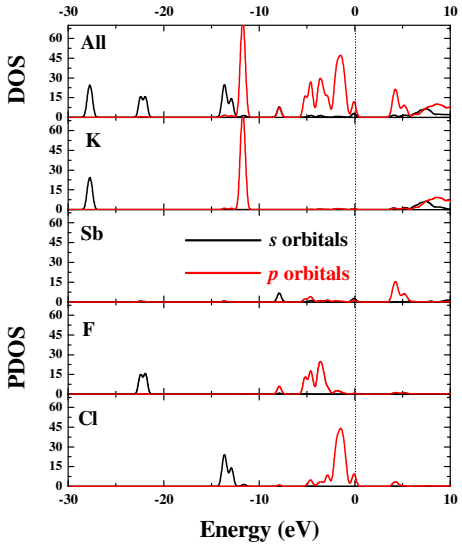

(a)

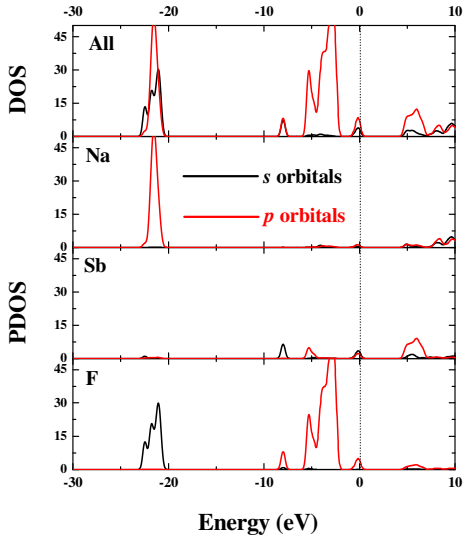

(b)

Fig. 7 DOS and PDOS plots of (a) $K_2SbF_2Cl_3$ and (b) Na_2SbF_5.

Optical response and real-space atom cutting

The calculated band gaps are 3.68 eV and 4.35 eV for $K_2SbF_2Cl_3$ and Na_2SbF_5, respectively, and both values are smaller than the experimental values of 4.01 eV and 5.0 eV. So scissors factors of 0.33 eV and 0.65 eV are used in the calculations of optical properties.

The first-principles linear and nonlinear optical properties in $K_2SbF_2Cl_3$ and Na_2SbF_5 at the wavelength of 1064 nm are listed in Table 3. Both crystals have relatively large optical birefringence which is enough to achieve the phase-matching condition for the SHG generation in the visible and IR spectral regions. Moreover, it is predicted that the non-zero independent SHG coefficient of $K_2SbF_2Cl_3$ is d_{36} = -2.03 pm/V (~ 5×KDP), more than 10 times larger than that in Na_2SbF_5 (d_{36} = -0.16 pm/V). Our calculated results are in good agreement with the experimental measurements (~ 4×KDP). The very different SHG effects in the two crystals evoke our interests since their structural feature is very similar except that three fluorine anions in each $[SbF_5]^{2-}$ group in Na_2SbF_5 are replaced by chlorine anions so as to form a $[SbF_2Cl_3]^{2-}$ group in $K_2SbF_2Cl_3$, and the potassium cations are replaced by sodium cations. Our real-space atom-cutting results (Table 4) reveal that actually the alkali earth cations (K^+ and Na^+) have very little contribution to the overall SHG effects, so the SHG effect difference between the two crystals are mainly resulted from the anionic groups. Indeed, the SHG coefficient of $[SbF_2Cl_3]^{2-}$ group in $K_2SbF_2Cl_3$ is about one order larger than that of $[SbF_5]^{2-}$ group in Na_2SbF_5, consistent with the ratio of the overall SHG effects in the two crystals. In order to investigate

difference between the electronic properties, we plotted the electronic charge density on the Sb-Cl and Sb-F bonds in $K_2SbF_2Cl_3$ (Fig. 8). Clearly, more charges are located on the Sb-Cl bonds than on the Sb-F bonds, indicating the much stronger covalent characteristic of the former chemical bonds where electrons can be perturbed more easily. Thus, the optical active covalent bonds in $[SbF_2Cl_3]^{2-}$ group significantly enhance the anisotropy of optical response in $K_2SbF_2Cl_3$ compared with the ionic bonds in $[SbF_5]^{2-}$ group and the much more prominent SHG effect in $K_2SbF_2Cl_3$ is mainly originated from the replacement of Cl anions at the F sites in the $[SbF_5]^{2-}$ groups in Na_2SbF_5.

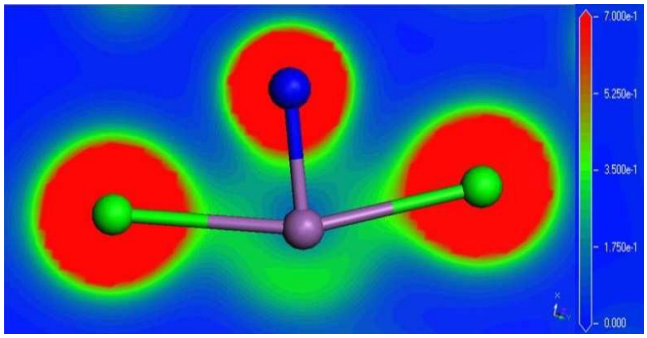

Fig. 8 The electronic charge density plotting on the Sb-Cl and Sb-F bonds in $K_2SbF_2Cl_3$. The antimony, chlorine and fluorine atoms are represented by purple, green and blue balls, respectively.

Table. 3 The first-principles linear and nonlinear optical coefficients in $K_2SbF_2Cl_3$ and Na_2SbF_5 at the wavelength of 1064nm.

	$K_2SbF_2Cl_3$	Na_2SbF_5
n_x	1.8843	1.5279
n_y	1.8853	1.5918
n_z	1.7689	1.587
Δn	0.1164	0.0639
d_{36}	-2.03 pm/V	-0.16 pm/V

Table. 4 The values of the SHG coefficients d_{36} for the contributions from the anionic groups and the sum of the anionic groups in a $K_2SbF_2Cl_3$(or Na_2SbF_5) cell, according to the results of the real-space atom cutting method.

	Without cations	Sum of the anionic groups
$K_2SbF_2Cl_3$	-2.02	-2.404
Na_2SbF_5	-0.17	-0.3389

Thermal properties

The thermal behavior of $K_2SbF_2Cl_3$ was investigated using thermogravimetric analysis (TGA). The TG curve reveals that it is thermally stable up to about 180 °C (Fig. 9). Its crystal is not hygroscopic and does not change its colour after being exposed to air for about a few months.

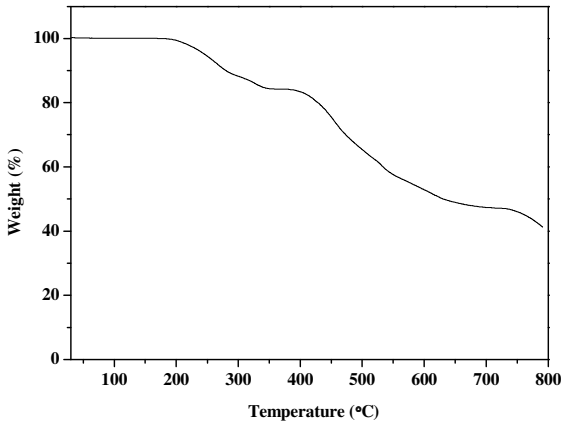

Fig. 9 The TG curve of $K_2SbF_2Cl_3$.

Conclusions

In summary, $K_2SbF_2Cl_3$, has been newly synthesized by hydrothermal reaction. It crystallizes in the NCS space group $P2_12_12_1$. The compound shows phase-matchable SHG effect of 4 times as strong as that of KDP. Its optical band gap is 4.01eV implying that it will exhibit much higher laser damage threshold than those commercialized IR NLO materials. And it also shows a wide transparent range (from 0.31 to 14μm) and a good thermal stability. Owing to these excellent comprehensive properties, $K_2SbF_2Cl_3$ appears to be a new candidate for NLO materials in the mid-IR region.

Acknowledgements

This work was supported by the National Science Foundation of China (Grant No. 91022036 and 11174297), the National Key Fundamental Research (973) Program of China (Grant No. 2010CB630701) and the National High Technology Research and Development (863) Program of China (Grant No. 2015AA034203).

Notes and references

1 D. M. Burland, R. D. Miller and C. A. Walsh, *Chem. Rev.*, 1994, **94**, 31.
2 (a) C. T. Chen, B. C. Wu, A. D. Jiang and G. M. You, *Sci. Sin. Ser. B*, 1985, **28**, 235; (b) C. T. Chen, Y. C. Wu, A. D. Jiang, B.

C. Wu, G. M. You, R. K. Li and S. J. Lin, *J. Opt. Soc. Am. B*, 1989, **6**, 616; (c) W. L. Smith, *Appl. Opt.*, 1977, **16**, 798; (d) K. Kato, *IEEE J. Quantum Electron.*, 1991, **27**, 1137; (e) G. D. Boyd, R. C. Miller, K. Nassau, W. L. Bond and A. Savage, *Appl. Phys. Lett*., 1964, **5**, 234.

3 (a) A. O. Okorogu, S. B. Mirov, W. Lee, D. I. Crouthamel, N. Jenkins, A. Y. Dergachev, K. L. Vodopyanov and V. V. Badikov, *Opt .Commun.*, 1998, **155**, 307; (b) D. S. Chemla, P. J. Kupecek, D. S. Robertson and R. C. Smith, *Opt. Commun.*, 1971, **3**, 29; (c) G. D. Boyd, H. M. Kasper, J. H. McFee and F. G. Storz, *IEEE J. Quant .Electron.*, 1972, **8**, 900; (d) G. D. Boyd, E. Buehler and F. G. Storz, *Appl. Phys. Lett*., 1971, **18**, 301.

4 (a)J. Zhang, N. Su, C. Yang, J. Qin, N. Ye, B. Wu and C. Chen, *Proc. SPIE.*, 1998, **1**, 3556;(b)P. Ren, J. Qin and C. Chen, *Inorg. Chem.*, 2003, **42**, 8; (c)G. Zhang, J. Qin, T. Liu, P. Fu, Y. Wu and C. Chen, *Opt. Mater.*, 2008, **31**, 110; (d)G. Zhang, J. Qin, T Liu, Y. Li, Y. Wu and C. Chen, *Appl. Phys. Lett*., 2009, **95**, 261104;(e)G. Zhang, J. Qin, T. Liu, P. Fu, Y. Wu and C. Chen, *Cryst. Growth Des.*, 2008, **8**, 2946; (f)T. Liu, G. Zhang, T. Zhu, F. Niu, J. Qin, Y. Wu and C. Chen, *Appl. Phys. Lett.*, 2008, **93**, 091102; (h)G. Zhang, Y. Li, K. Jiang, H. Zeng, T. Liu, X. Chen, J. Qin, Z. Lin, P. Fu, Y. Wu and C. Chen, *J. Am. Chem. Soc.*, 2012, **134**, 14818; (i)Y. Li, M. Wang, T. Zhu, X. Meng, C. Zhong, X. Chen and J. Qin, *Dalton Trans.*, 2012, **41**, 763; (j)Q. Wu, Y. Li, H. Chen, K. Jiang, H. Li, C. Zhong, X. Chen and J. Qin, *Inorg. Chem. Commun.* , 2013, **34**, 1; (k)Y. Huang, X. Meng, L. Kang, Y. Li, C. Zhong, Z. Lin, X. Chen and J. Qin, *CrystEngComm*, 2013, **15**, 4196; (l)Y. Dang, X. Meng, K. Jiang, C. Zhong, X. Chen and J. Qin, *Dalton Trans.*, 2013, **42**, 9893.1; (m)Q. Wu, X. Meng, C. Zhong, X. Chen and J. Qin, *J. Am. Chem. Soc.*, 2014, **136**, 5683;(n) X. M. Jiang, M. J. Zhang, H. Y. Zeng, G. C. Guo and J. S. Huang, *J. Am. Chem. Soc.*, 2011, **133**, 3410.

5 (a) L. A. Zemnukhova, A. A. Udovenko, Yu. E. Gorbunova, G. A. Fedorishcheva, Yu. N. Mikhailov and R. L. Davidovich, *Russ. J. Coord. Chem.*, 1998, **24**, 781; (b) L. A. Zemnukhova and G. A. Fedorishcheva, *Russ. Chem. Bull.*, 1999, **48**, 104;(c) R. Fourcade, G. Mascherpa, E. Philippot, M. Maurin, *Revue de ChimieMinerale*, 1974, **11**, 481;(d) J. Bergman, D. Chemla, R. Fourcade, G. Mascherpa, , *J. Solid State Chem.* , 1978, **23**, 187;(e) K. Wu and C. Chen, *Appl. Phys.* , 1992, **A54**, 209;(f) K. Wu, C. Chen, *J. Cryst. Growth*, 1996, **166**, 533;(g) Y. Tong, X. Meng, Z. Wang, C. Chen, and M. Lee, *J. Appl. Phys.*, 2005, **98**, 033504.

6 P. M. Kubelka and F. Z. Munk, *Tech. Phys.*, 1931, **12**, 593.

7 S. K. Kurtz and T. T. Perry, *J. Appl. Phys.*, 1968, **39**, 3798.

8 G. M. Sheldrick, *SHELXTL, Version 6.14*,Bruker Analytical X-ray Instruments, Inc., Madison, WI, USA, 2003.

9 G. M. Sheldrick, ActaCrystallogr., Sect. A: Found. Crystallogr., 2008, **A64**, 112.

10 M. C. Payne, M. P. Teter, D. C. Allan, T. A. Arias and J. D. Joannopoulos, *Rev. Mod. Phys.*, 1992, **64**, 1045.

11 S. J. Clark, M. D. Segall, C. J. Pickard, P. J. Hasnip, M. J. Probert, K. Refson and M. C. Payne, *Z. Kristallogr.*, 2005, **220**, 567.

12 P. Hohenberg and W. Kohn, *Phys. Rev.*, 1964, **136**, B864.

13 J. S. Lin, A. Qteish, M. C. Payne and V. Heine, *Phys. Rev. B: Condens. Matter Mater. Phys.*, 1993, **47**, 4174.

14 W. Kohn and L. J. Sham, *Phys. Rev.*, 1965, **140**, A1133.

15 H. J. Monkhorst and J. D. Pack, *Phys. Rev. B: Solid State*, 1976, **13**, 5188.

16 (a) C. S. Wang and B. M. Klein, *Phys. Rev. B: Condens. Matter Mater. Phys.*, 1981, **2**, 3393; (b) R. W. Godby, M. Schluter and L. J. Sham, *Phys. Rev. B:Condens. Matter Mater. Phys.*, 1988, **37**, 10159.

17 E. D. Palik, *Handbook of Optical Constants of Solids*, Academic Press, 1985, p. 190.

18 (a) J. Lin, M. H. Lee, Z. P. Liu, C. T. Chen and C. J. Pickard, *Phys. Rev. B:Condens. Matter Mater. Phys.*, 1999, **60**, 13380; (b) Z. S. Lin, J. Lin, Z. Z. Wang, Y. C. Wu, N. Ye, C. T. Chen and R. K. Li, *J. Phys.: Condens. Matter*, 2001, **13**, R369.

19 M. H. Lee, C. H. Yang and J. H. Jan, Phys. *Phys. Rev. B: Condens. Matter Mater. Phys.*, 2004, **70**, 235110.

20 C. T. Chen, T. Sasaki, R. K. Li, Y. C. Wu, Z. S. Lin, Y. Mori, Z. G. Hu, J. Y. Wang, G. Aka, M. Yoshimura and Y. Kaneda, *Nonlinear Optical Borate Crystals*, Wiley-VCH, Germany, 2012.